

On-Chip Single Plasmon Detection

Reinier W. Heeres,^{*,†} Sander N. Dorenbos,[†] Benny Koene,[†] Glenn S. Solomon,[‡]
Leo P. Kouwenhoven,[†] and Valery Zwiller[†]

[†]Kavli Institute of Nanoscience, Delft University of Technology, P.O. Box 5046, 2600 GA Delft, The Netherlands, and

[‡]Joint Quantum Institute, NIST and University of Maryland, 100 Bureau Drive MS-8423, Gaithersburg, Maryland 20899-8423

ABSTRACT Surface plasmon polaritons (plasmons) have the potential to interface electronic and optical devices. They could prove extremely useful for integrated quantum information processing. Here we demonstrate on-chip electrical detection of single plasmons propagating along gold waveguides. The plasmons are excited using the single-photon emission of an optically emitting quantum dot. After propagating for several micrometers, the plasmons are coupled to a superconducting detector in the near-field. Correlation measurements prove that single plasmons are being detected.

KEYWORDS Single surface plasmons, superconducting detectors, semiconductor quantum dots, nanophotonics

The term *plasmons* refers to light confined to a metal/dielectric interface, with appealing characteristics of shortened wavelengths and enhanced field strengths.¹ Plasmons are also easily guided on-chip over distances of many micrometers. Most interest has been in the classical, many-photon regime where plasmons are generated by light and after traveling along the metal surface, re-emitted as photons into free space. A few experiments with respect to quantum properties have been performed. First, it was shown that the plasmon-mediated enhanced light transmission through arrays of holes in a metal surface conserves the photon's polarization properties, including quantum superpositions.² Similar work showed that energy–time entanglement is also preserved.³ Second, it was shown that coupling single emitters to silver nanowires in the near-field allows excitation of single plasmons.^{4,5} All these schemes relied on conversion of the plasmon to a free photon and subsequent far-field detection with traditional single photon detectors. Alternatively, on-chip electrical detection has been demonstrated using organic photo-diodes,⁶ gallium arsenide structures⁷ and germanium wires.⁸ However, none of these techniques has provided single plasmon sensitivity. By coupling a plasmon waveguide to a superconducting single-photon detector (SSPD), we demonstrate on-chip electrical detection of single plasmons. Next to single-photon sensitivity,⁹ this on-chip, near-field detection has the potential for high detection efficiency, large bandwidth, and low timing jitter.

Our SSPDs consist of a meandering NbN wire ($\sim 100 \mu\text{m}$ long, 100 nm wide, $\sim 5 \text{ nm}$ thin). The critical temperature T_c below which the wire becomes superconducting is approximately 9 K . When applying a bias current close to the critical current, absorption of a single photon is sufficient to create a local region in the normal, resistive state. This short-

lived resistive state is detected as a voltage pulse at the terminals of the wire. The excess energy is dissipated within a fraction of a nanosecond, after which the superconducting state can be restored. The detection rate is limited by the kinetic inductance of the superconducting wire,¹⁰ which in our current detectors gives a maximum count rate of 100 MHz . As we show here, this detection mechanism can also efficiently measure individual plasmons.

We fabricate plasmon waveguides from polycrystalline gold strips, which are electrically insulated from the NbN by a thin dielectric (Figure 1a, Supporting Information). Gratings at both ends serve to couple incoming free-space photons to plasmons confined to the bottom gold/dielectric interface.¹¹ These plasmons propagate to the detector where they are absorbed and detected (Figure 1b).

Measurements are performed in a cryostat at $\sim 4 \text{ K}$ with the sample mounted on an XYZ translation stage. A laser is focused through a cold microscope objective, and a count-rate XY-map is measured as a function of laser-spot position. We find a large detector response when the laser directly illuminates the SSPD (three peaks at $X \approx 11 \mu\text{m}$ in parts c and d of Figure 1). The detector response is very low with the laser spot on the substrate or gold strip, except at the grating regions. These detector peaks (consistently shifted for waveguides 1 and 2, Figure 1c) show that light converted to plasmons is detected electrically on-chip.

To substantiate the electrical detection of plasmons, we have performed several checks. First, we measured one waveguide with an intentional $1 \mu\text{m}$ gap between grating and detector (Figure S1 in Supporting Information), resulting in a strong suppression of the detector signal. Second, we rotated the incoming light polarization and retrieve a proper polarization-dependent detector signal (Figure S2 in Supporting Information). We further measured wavelength dependence and find a vanishing signal at $\sim 650 \text{ nm}$ due to losses in the gold film and a rapidly increasing detector response for longer wavelengths. Finally we measured the

* Corresponding author, r.w.heeres@tudelft.nl.

Received for review: 11/10/2009

Published on Web: 12/30/2009

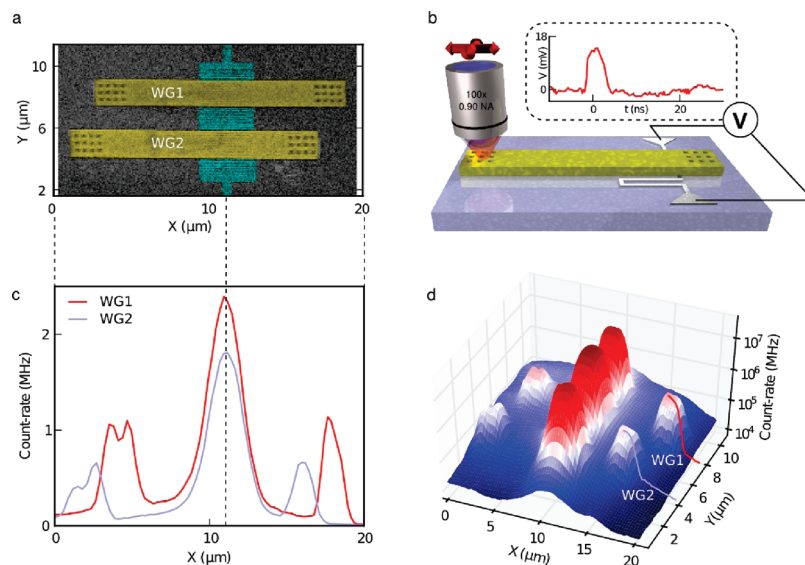


FIGURE 1. (a) A scanning electron microscopy image showing the superconducting detector (cyan) and two gold waveguides (yellow) with coupling gratings. (b) Representation of the low-temperature setup. The sample is XY-scanned through the laser focus. Illumination of the grating excites plasmons at the substrate/gold interface. After propagating along the waveguide, absorption in the SSPD gives a voltage pulse, V . (c) SSPD pulse counts versus laser-spot position. (d) 2D XY-scan. The blue and red lines (WG1 and WG2) indicate where the line-cuts in (c) are taken.

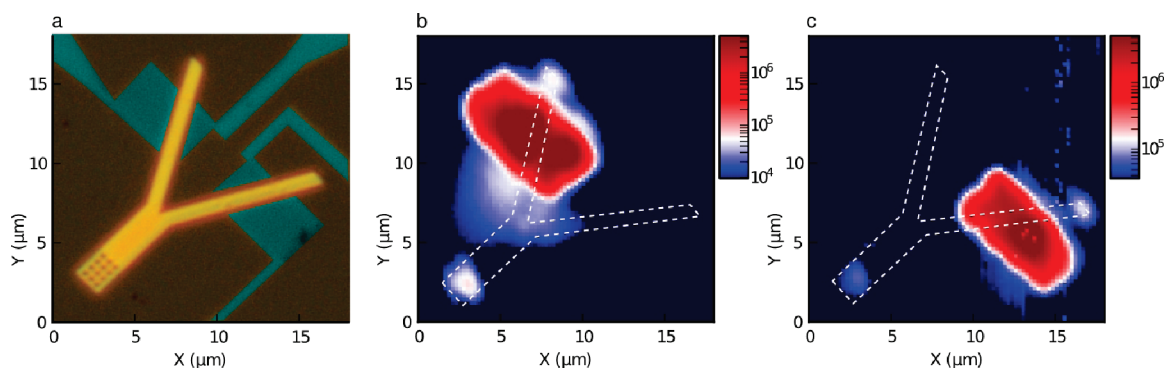


FIGURE 2. (a) Microscope image of a plasmon Y-splitter device. The SSPDs (cyan) are colorized. (b, c) Signal of the left (b) and right (c) detector when scanning a laser spot (980 nm) across the device in (a). Just one detector produces a signal when illuminating the left or right detector. Both detectors produce a signal when illuminating the grating on the bottom left, indicating that plasmons couple to both arms of the Y-splitter. The white contours of the waveguide are a guide to the eye. Note that the color scales are different due to different dark-count levels in the left and right detectors.

plasmon decay length in our gold strips and find a $1/e$ -decay of $\sim 10 \mu\text{m}$ for 810 nm light. All these checks are in qualitative agreement with simulations using Lumerical FDTD software.

We have fabricated several waveguides with varying grating-detector distances and shapes (e.g., a bend, Figure S1 in Supporting Information). We also designed more complex structures to illustrate the flexibility of our fabrication method, one of which is a Y-splitter (Figure 2a). Again the experiment consists of scanning a laser beam across the sample. In this case, the count rates of the left (Figure 2b) and the right (Figure 2c) detectors are monitored simultaneously. Next to the individual detectors, which are visible in just one of the signals, the grating in the bottom left is visible in both images. This indicates that plasmons excited at the grating are propagating in both arms of the Y structure.

This device could be used as an integrated plasmon Hanbury Brown and Twiss interferometer. The splitter is designed to be symmetric and therefore balanced. However, because the efficiency of the individual detectors is determined by their intrinsic sensitivity (e.g., microscopic properties) and the applied bias current, it is not possible to measure the absolute splitting ratio in this configuration. Our current plasmon waveguides are all multimode, but in the future they can be downsized to single-mode structures implementing interference-based devices such as Mach-Zehnder interferometers¹² and coincidence-based quantum logic gates¹⁵ using plasmons.

SSPDs are well characterized and proven to have single photon sensitivity.⁹ The power dependence (Figure S3 in Supporting Information) already strongly suggests single plasmon sensitivity, since it is linear even in the regime

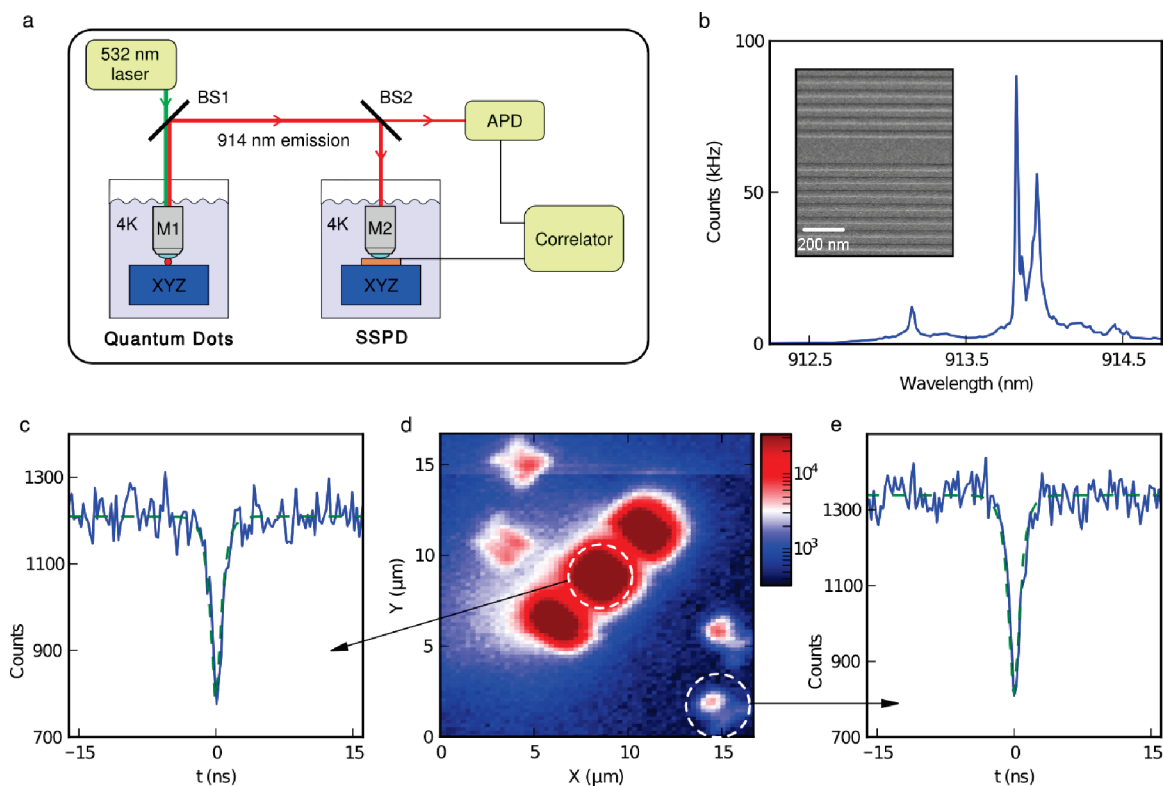


FIGURE 3. (a) Schematic representation of the measurement setup. Quantum dots and SSPD are cooled to 4 K in two separate cryostats, which are coupled free-space. BS1 and BS2 are both beamsplitters transmitting 10% and reflecting 90% of the incoming beam. The microscope objectives M1 and M2 are $60\times$, 0.85 NA and $100\times$, 0.90 NA, respectively. (b) Spectrum of a single SK quantum dot and a scanning electronic microscopy image of the distributed Bragg reflector (inset). (c) Time-correlation measurement with 10% of the quantum dot emission going to an APD and 90% sent directly to the SSPD. The integration time is 33 min, fitted normalized depth 0.46, and lifetime 655 ps. (d) Counts of the SSPD (same device design as Figure 1a) as a function of focus position of the emission from the quantum dot in (b). The dashed circles indicate the positions where the correlation measurements in (c) and (e) are taken. (e) Time-correlation measurement with 90% of the light sent to the grating on the bottom right. The dip at $t = 0$ ns confirms that the photon statistics are maintained after photons are converted into plasmons. The integration time is 8 h, fitted normalized depth 0.50, and lifetime 708 ps.

where the average number of incoming photons within the detector dead time (~ 10 ns) is much smaller than 1. However, to unambiguously prove single plasmon sensitivity requires a single photon source for plasmon excitation in addition to a time-correlation measurement.⁴ We performed this measurement by cooling Stranski–Krastanov (SK) quantum dots (QDs) in a second cryostat. This sample contains QDs at the center of a distributed Bragg reflector microcavity (Figure 3b, inset) to enhance the brightness.¹⁴ The emission of one of these QDs is collected and sent through a narrow bandpass filter. The filtered spectrum is shown in Figure 3b. Ten percent of this emission is collected in an optical fiber and sent to an avalanche photodiode (APD). The other 90% is coupled through free-space to the setup containing the SSPD with waveguides (Figure 3a). To confirm that we are looking at a single-photon source, we first position the incoming beam directly at the SSPD. The correlation measurement between detection events from the APD and the SSPD is shown in Figure 3c. An antibunching dip with a fitted depth close to 0.5 is clearly visible. The fact that the dip does not go below the theoretical limit of 0.5 for a single emitter is likely to be due to background emission from the substrate

and nonperfect filtering, especially since the two main peaks in the spectrum only constitute $\sim 60\%$ of the total counts.

The next step is to perform another XY-scan using the single photons from the QD (Figure 3d). This scan clearly confirms that single plasmons can be excited by illuminating the gratings with single photons. After focusing the emission of the single-photon source on the lower-right grating, another correlation measurement is performed between the APD and the SSPD. The SSPD now detects plasmons that have propagated about $7.5\ \mu\text{m}$ along the waveguide after coupling in through the grating. The resulting data clearly show that the quantum statistics of the original photons are maintained and that single plasmons are being detected. This is the first time that single plasmons are observed on-chip in the near-field and opens up a wide range of possibilities in quantum plasmonics. By placing a single emitter on-chip using nanomanipulation,¹⁵ the integration could even be taken one step further, resulting in a complete optical circuit with efficient coupling of a single-photon source^{16,17} to a waveguide and a detector on a monolithic device.

Detecting single plasmons on-chip makes our waveguide-detector scheme very promising for ultrafast detection

with low dark-count rates. The time resolution of <70 ps that can be achieved with an SSPD today is comparable to the best APDs. However, contrary to those detectors the SSPDs also provide good sensitivity in the near-infrared range, up to several micrometers in wavelength. Combined with the flexibility for fabricating various complex waveguide structures, this results in many potential applications as sensors or interconnects and for quantum information processing.

Acknowledgment. We thank Ewold Verhagen and Freek Kelkensberg for discussions and Nika Akopian for support. This work is supported financially by The Netherlands Organisation for Scientific Research (NWO/FOM).

Supporting Information Available. Materials and methods (fabrication, measurement setup, quantum dots, fitting details) and additional device geometries and measurements (2D scan, power dependence, polarization dependence). This material is available free of charge via the Internet at <http://pubs.acs.org>.

REFERENCES AND NOTES

- (1) Barnes, W. L.; Dereux, A.; Ebbesen, T. W. *Nature* **2003**, *424*, 824–830.
- (2) Altewischer, E.; Van Exter, M. P.; Woerdman, J. P. *Nature* **2002**, *418*, 304–306.
- (3) Fasel, S.; Robin, F.; Moreno, E.; Erni, D.; Gisin, N.; Zbinden, H. *Phys. Rev. Lett.* **2005**, *94*, 110501.
- (4) Akimov, A. V.; Mukherjee, A.; Yu, C. L.; Chang, D. E.; Zibrov, A. S.; Hemmer, P. R.; Park, H.; Lukin, M. D. *Nature* **2007**, *450*, 402–406.
- (5) Kolesov, R.; Grotz, B.; Balasubramanian, G.; Stöhr, R. J.; Nicolet, A. A. L.; Hemmer, P. R.; Jelezko, F.; Wrachtrup, J. *Nat. Phys.* **2009**, *5*, 470–474.
- (6) Ditlbacher, H.; Aussenegg, F. R.; Krenn, J. R.; Lamprecht, B.; Jakopic, G.; Leising, G. *Appl. Phys. Lett.* **2006**, *89*, 161101.
- (7) Neutens, P.; Van Dorpe, P.; De Vlaminc, I.; Lagae, L.; Borghs, G. *Nat. Photonics* **2009**, *3*, 283–286.
- (8) Falk, A. L.; Koppens, F. H. L.; Yu, C. L.; Kang, K.; de Leon Snapp, N.; Akimov, A. V.; Jo, M. H.; Lukin, M. D.; Park, H. *Nat. Phys.* **2009**, *5*, 475–479.
- (9) Gol'tsman, G. N.; Okunev, O.; Chulkova, G.; Lipatov, A.; Semenov, A.; Smirnov, K.; Voronov, B.; Dzardanov, A.; Williams, C.; Sobolewski, R. *Appl. Phys. Lett.* **2001**, *79*, 705.
- (10) Kerman, A. J.; Dauler, E. A.; Keicher, W. E.; Yang, J. K. W.; Berggren, K. K.; Gol'tsman, G. N.; Voronov, B. *Appl. Phys. Lett.* **2006**, *88*, 111116.
- (11) Verhagen, E.; Polman, A.; Kuipers, L. *Opt. Express* **2008**, *16*, 45–57.
- (12) Bozhevolnyi, S. I.; Volkov, V. S.; Devaux, E.; Laluet, J. Y.; Ebbesen, T. W. *Nature* **2006**, *440*, 508–511.
- (13) Politi, A.; Cryan, M. J.; Rarity, J. G.; Yu, S.; O'Brien, J. L. *Science* **2008**, *320*, 646–649.
- (14) Solomon, G. S.; Pelton, M.; Yamamoto, Y. *Phys. Rev. Lett.* **2001**, *86*, 3903–3906.
- (15) van der Sar, T.; Heeres, E. C.; Dmochowski, G. M.; de Lange, G.; Robledo, L.; Oosterkamp, T. H.; Hanson, R. *Appl. Phys. Lett.* **2009**, *94*, 173104.
- (16) Chang, D. E.; Sørensen, A. S.; Hemmer, P. R.; Lukin, M. D. *Phys. Rev. Lett.* **2006**, *97*, 053002.
- (17) Chang, D. E.; Sørensen, A. S.; Demler, E. A.; Lukin, M. D. *Nat. Phys.* **2007**, *3*, 807–812.